

## Influence on the secondary electron yield of the space charge induced in an insulating target by an electron beam

This article has been downloaded from IOPscience. Please scroll down to see the full text article.

1998 J. Phys.: Condens. Matter 10 5821

(<http://iopscience.iop.org/0953-8984/10/26/010>)

View [the table of contents for this issue](#), or go to the [journal homepage](#) for more

Download details:

IP Address: 171.66.16.209

The article was downloaded on 14/05/2010 at 16:34

Please note that [terms and conditions apply](#).

# Influence on the secondary electron yield of the space charge induced in an insulating target by an electron beam

R Renoud<sup>†</sup>, C Attard<sup>†</sup>, J-P Ganachaud<sup>†</sup>, S Bartholome<sup>‡</sup> and A Dubus<sup>‡§</sup>

<sup>†</sup> Equipe de Physique des Solides pour l'Electronique EA 1153, Laboratoire de Physique du Solide Théorique, Faculté des Sciences et des Techniques de l'Université de Nantes, 2 Rue de la Houssinière, BP 92208, 44322 Nantes Cedex 03, France

<sup>‡</sup> Université Libre de Bruxelles, Service de Métrologie Nucléaire (CP 165), Avenue F D Roosevelt 50, B-1050 Brussels, Belgium

Received 28 April 1998

**Abstract.** The building up of the space charge induced by electron bombardment in an insulating target is due to the stabilization of self-trapped electrons and holes in polaronic traps. For the energies considered, the target charges positively and the secondary electrons emitted at low energies can be attracted back to the surface. This results in a self-regulation effect where the total secondary yield tends to unity and the surface potential stabilizes at a low positive value. This conclusion is checked for various experimental conditions. The electrons landing on the target form a ring of negative charges that progressively spread out on the surface of the sample.

## 1. Introduction

In the present paper we focus on the secondary electron emission of insulating targets induced by electron bombardment. The initial 'source' of secondary electrons is due to the primary beam, but the elementary processes which govern the subsequent transport of the charges are indeed common to all the physics of insulators.

The secondary electron emission is the result of a cascade effect involving particles with energies varying from that of the primary beam down to a fraction of eV. Moreover, in an insulating medium, the low energy charge carriers are strongly influenced by the polarization effects. The basic concepts used in the present study to explain the building up of the space charge are the formation of polarons, their diffusion under the influence of the internal field and their subsequent fixation into traps.

## 2. Electron–insulator interaction model

### 2.1. Collisions

The interaction model used in this work has already been presented in several publications [1, 2] and we shall only recall it briefly.

It is generally admitted (see [3]) that the elastic interaction of an electron with the potential surrounding the ionic cores is correctly described by the partial-wave method.

§ Chercheur qualifié FNRS.

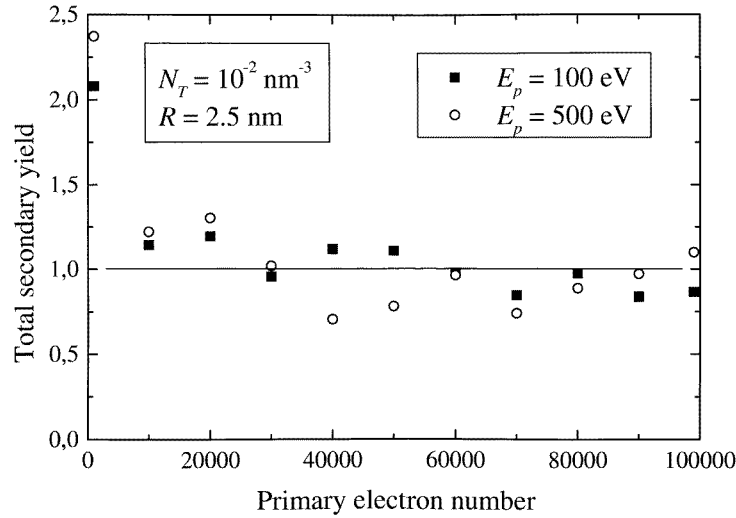


**Figure 1.** Evolution of the total secondary emission yield during the charge for two primary energies.

In an insulator, the energy losses suffered by the electrons are essentially due to the collisions with the electrons of the valence band. They are taken into account by the dielectric theory (see [4, 5] for instance). Moreover, when its energy is sufficiently high, an electron can also cause the ionization of an inner shell. This process is taken into account by the classical formalism of Gryzinski [6].

The interaction of a low energy electron (up to a few tenths of an eV) with the longitudinal optical phonon mode (LO) is described by Fröhlich's formalism [7]. We have taken into account the possibility for an electron either to create or to absorb a longitudinal optical phonon in such a collision. The formalism developed by Bradford and Woolf [8] and the extensions proposed by Akkerman *et al* [9] have been retained for the interactions of the electrons with the longitudinal and transverse acoustic phonons (LTA). These collisions involve small energy transfers but give rise to important angular deflections. Moreover their probability is high, of the order of that of elastic collisions with the ionic cores.

## 2.2. Insulator polarization and space charge

A low energy charge carrier moving in an insulating medium is submitted to polarization effects. This interaction is responsible for an increase of the effective mass of the carrier and can lead, at least partially, to its localization by formation of a polaron [10–13]. In our model, we have retained a phenomenological approach to account for the formation of a polaron by a low energy electron. The probability per unit path length, for an electron of energy  $E$ , is given by:

$$P_{pol}(E) = S_{pol} \exp(-\gamma_{pol} E) \quad (1)$$

where the parameter  $S_{pol}$  fixes the spatial frequency of the process and the constant  $\gamma_{pol}$  limits the energy domain concerned by these polarization effects. For a hole, the approach which has been retained here, is still simpler as we assume that the formation of a polaron takes place immediately.

Under the influence of the internal electric field, a polaron diffuses along the field lines. This diffusion is taken into account by assigning a mobility to the charge carrier (much higher for an electron than for a hole due to their different effective masses). The polaron can be stabilized when it encounters a trapping site. We shall assume here that the diffusion distance covered by a polaron before being trapped,  $L_{trap}$ , follows an exponential law. The corresponding trapping mean free path  $\lambda_{trap}$  is taken as constant, the same for an electron or for a hole and does not depend on the polaron energy.

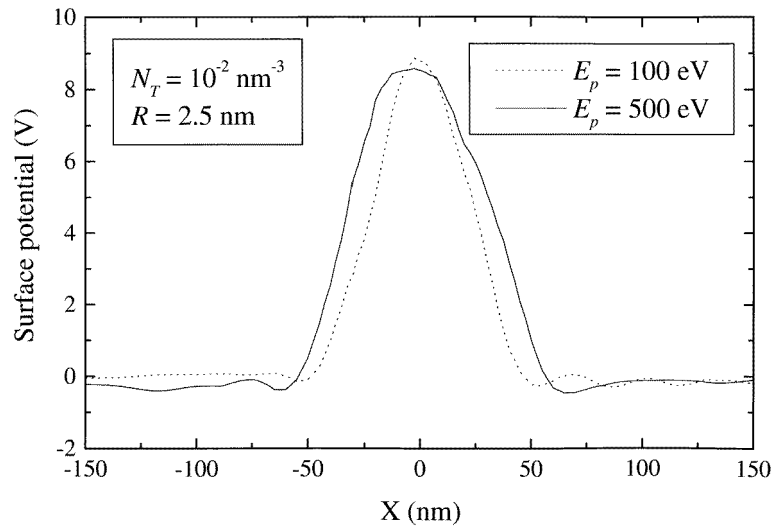


**Figure 2.** Surface potential distribution for two primary energies.

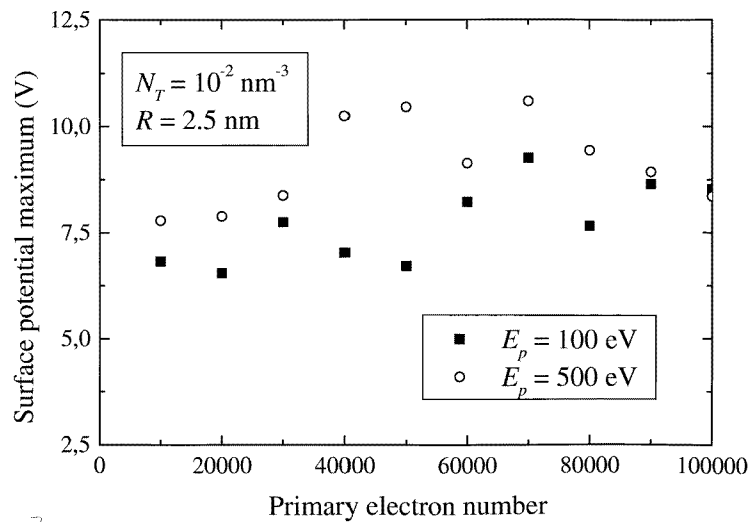


**Figure 3.** Variation of the maximum of the surface potential during the charge for two primary energies.

In an insulating target, the trapping sites may be of quite different types (charged or neutral impurities, dislocations, grain boundaries, . . .). It is out of the scope of the present paper to account precisely for the nature of these traps. Due to the complexity of the problem, we shall use here a very simplified model. It has been assumed that the traps were uniformly distributed in the bulk of the insulator. The sites able to fix the holes do not have to be distinguished from others able to fix the electrons; in practice, they play equivalent roles. Their densities are equal, and both types of site are sufficiently close together to allow a recombination to take place. When a carrier encounters an empty trap, it becomes fixed there; if a carrier having an opposite charge already occupies the trap, a recombination takes place; if the trap is occupied by a carrier having an identical charge, exclusion effects force the polaron to diffuse.

In practice, the solid has been divided into cubic cells. Each cell contains one trapping site (hence its volume depends on the trap density). For more details on diffusion and trapping, see [1, 2]. No subsequent detrapping processes have been explicitly taken into account in this model. We are presently working on this problem.

### 3. Results for the charge of an insulating target subjected to a well focused low energy electron beam

The simulation of the charge transport is made by the Monte Carlo method. The calculation of the electric field due to the trapped charges is performed self-consistently. Statistical estimations can be made at various stages of the formation of the internal charge. Moreover, the simulation code allows keeping track, in a quasi temporal way, of the processes that contribute to the charge.

Our model is quite general but at very low energies the various scattering cross-sections probably become less reliable. For this reason, it is not very reasonable to extend the calculations to primary energy values below 50 eV. Moreover, this domain has not been much studied experimentally. At high energies (beyond a few keV for instance), our Monte Carlo model as it stands would require a much too long computational time. In this energy domain simplified simulation codes have to be considered.

The parameters used for the present study are representative of an SiO<sub>2</sub> target, but the crystalline structure of the sample has not been taken into account. This sample is assumed to be semi-infinite and to present a density  $N_T$  of active traps of  $10^{-2}$  per nm<sup>3</sup>. The target is irradiated at normal incidence by a well focused electron beam. The density of current in the primary spot follows a Gaussian law on the surface, with a standard deviation  $R = 2.5$  nm. We have simulated the arrival of one electron every 100 fs. This corresponds to a total intensity of 1  $\mu$ A and a density of current of  $10^7$  A cm<sup>-2</sup>. The energy  $E_p$  of the beam is situated between the two critical energies  $E_{C1}$  and  $E_{C2}$ , for which the conventional secondary emission yield is equal to the unity. These values are located at about 50 eV and 2700 eV respectively for SiO<sub>2</sub> [14–16]. So, in the present study, the secondary emission yield will always exceed unity, at least in the first stage of the charge of the sample. From a preliminary study of the secondary electron yield of SiO<sub>2</sub> made for a large set of primary energies, a reasonable range of values could be deduced for  $S_{pol}$  and  $\gamma_{pol}$ . For the present calculations  $S_{pol} = 2$  nm<sup>-1</sup> and  $\gamma_{pol} = 0.5$  eV<sup>-1</sup> [17, 18]. Hugues [19] has proposed some values for the mobilities of low energy charge carriers in SiO<sub>2</sub>. By reference to this study, we have chosen  $\mu_e = 15$  cm<sup>2</sup> V<sup>-1</sup> s<sup>-1</sup> for the polaron formed by an electron. The value  $\mu_h = 0.1$  cm<sup>2</sup> V<sup>-1</sup> s<sup>-1</sup> has been taken for a hole in order to account for its higher effective mass. We have chosen  $\lambda_{trap} = 5$  nm for the trapping mean free path.

### 3.1. General characteristics of the space charge

The analysis of the distribution of the space charge built up in an  $\text{Al}_2\text{O}_3$  target by a low energy electron beam has already been presented elsewhere [1, 2]. The overall behaviour is indeed the same for  $\text{SiO}_2$  and here we shall just recall the main conclusions which had been previously obtained.

The charge of the target is globally positive. However, the spatial distribution of the charge changes with the irradiation time because the electrons and the holes, which have formed polarons, diffuse. Their mobilities are different. At the first stages of the simulation, transient effects can be observed under the primary beam impact, where electron pockets remain present in a region in majority positive. Afterwards, a stationary state occurs. The higher the mobilities are the more rapidly it is reached. Due to the progressive saturation of the traps, the polarons diffuse farther and farther before they are trapped: the charge distribution spreads out in the sample.

It is clear that these characteristics are quite general, however the charge distribution is sensitive to the experimental conditions. The penetration of the primary beam increases with the energy  $E_p$  and the transient effects persist all the longer as the primary energy is high. The spreading of the diffusion zone increases with the creation rate of the electron hole pairs that is to say with the yield. Quite evidently, the size of the diffusion zone augments when the density of traps decreases. The kinetics of the space charge formation depends also on the values of the carrier mobilities, which themselves depend on the material studied.

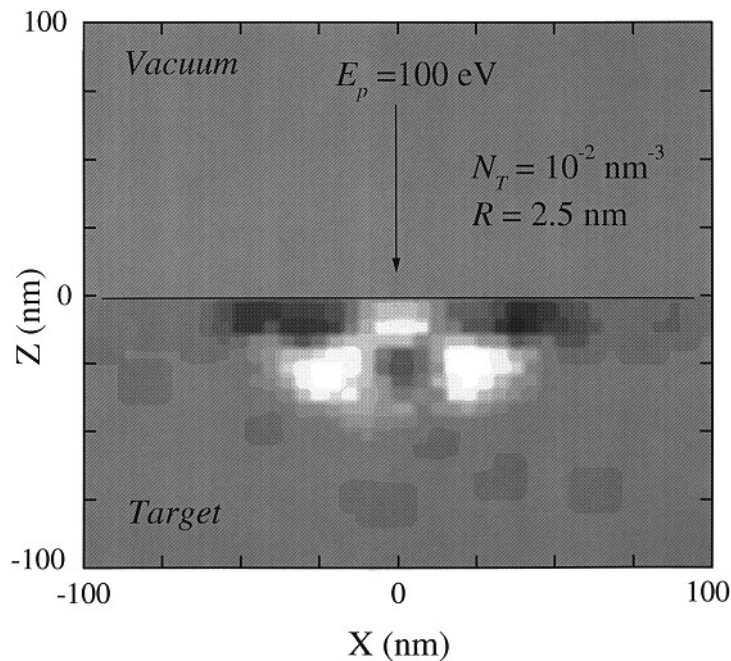


**Figure 4.** Distribution of the trapped charges for a simulation of 100 000 primary electrons and  $E_p = 100$  eV. The positively charged regions are shown in white, the negatively charged ones in black (and the uncharged regions in grey).

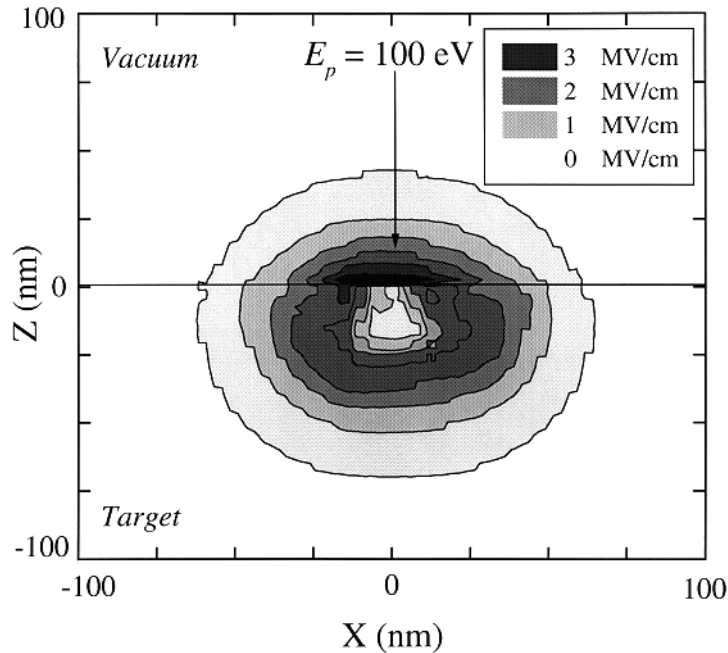


**Figure 5.** Modulus of the electrostatic field. The grey scale represents the intensity of the field.

### 3.2. Effects of the electrons attracted back

**3.2.1. Secondary yield and surface potential.** The trajectories of the secondary electrons emitted in the vacuum are strongly influenced by the field outside the target. The low energy electrons are driven back to the sample. This results in a reduction of the secondary yield. Figure 1 shows that the secondary yield decreases continuously when the number of simulated primary trajectories increases and tends to stabilize at a value close to unity. The electrons attracted back to the surface gives rise to a regulating effect. As the yield exceeds unity, the surface is positively charged. The driving back of electrons to the surface lowers the yield. One understands that this regulating effect will persist until the yield reaches unity. Then, for each electron impinging on the target, only one electron is emitted. Globally, no additional charge is trapped in the target and each electron–hole pair generated in the cascade will be subsequently neutralized: the system becomes stable. This is indeed what we calculated for all the primary energies for which our simulations have been made (figure 1).

One can also notice that the spatial distribution of the surface potential  $V_s$  attains a stable shape and presents a maximum of few eV in the primary spot region (figure 2). This is true for all the primary energies  $E_p$  in the range considered in the present study. Figure 3 shows the evolution of the maximum of  $V_s$  with the size of the sample of simulated primary electrons. The surface potential and the secondary emission yield are related quantities. The more  $V_s$  increases, the larger is the number of electrons attracted back to the surface. Finally the number of the holes which are not compensated by electrons decreases: the surface potential increases but at a much slower rate. So both quantities tend to their asymptotic values representative of the system in equilibrium.

Cazaux *et al* [20] have experimentally observed this kind of behaviour for an MgO target

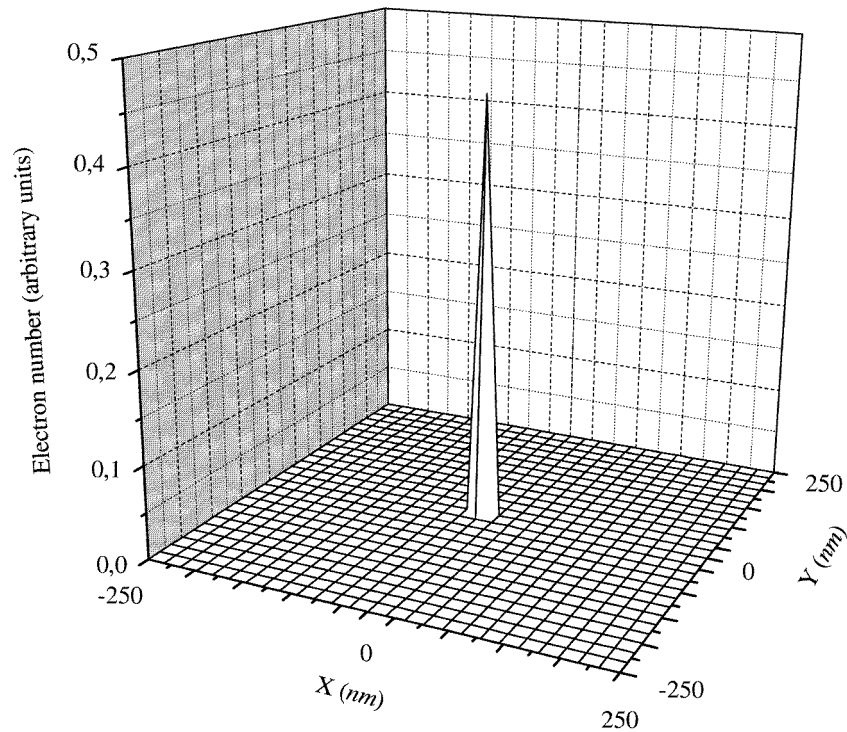


**Figure 6.** Spatial distribution of the secondary electrons emitted at the surface.

bombarded by a primary electron beam of energy in the range 1–4 keV. The effective yield was found to be close to unity and the surface potential to stabilize at a low value ( $0 \pm 2$  eV). General considerations on the charge of insulators induced by electron bombardment can be found in several other papers by Cazaux ([21] for instance).

**3.2.2. Charge distributions.** The distributions of the charges (positive or negative) behave as indicated above in our general discussion. As the time runs, the positive charges diffuse in the target under the influence of the internal field and they can reach more and more distant regions. Nevertheless, one can observe two phenomena related to the existence of a field outside the sample (figure 4). As the emitted electrons are attracted back by the positively charged sample, they contribute to the formation of a layer of negative charges close to the surface, except under the primary beam. This layer tends to reinforce itself along the primary bombardment and to form a ‘ring’ distribution. One also notices the formation of an electron pocket at the centre of the positively charged zone that has been created under the beam. In this region, the electric field is nearly null (figure 5) and the carriers cannot diffuse. In its neighbourhood, the global electric field is divergent. This prevents the positive charges from being attracted by the electrons of the pocket and recombining with them.

The emission of the secondary electrons concerns a narrow region of the surface of the target (figure 6). The emission zone is quite stable all along the bombardment. It is indeed representative of the domain where most of the inelastic interactions take place. This ‘mixing’ zone is determined by the primary beam penetration and practically does not



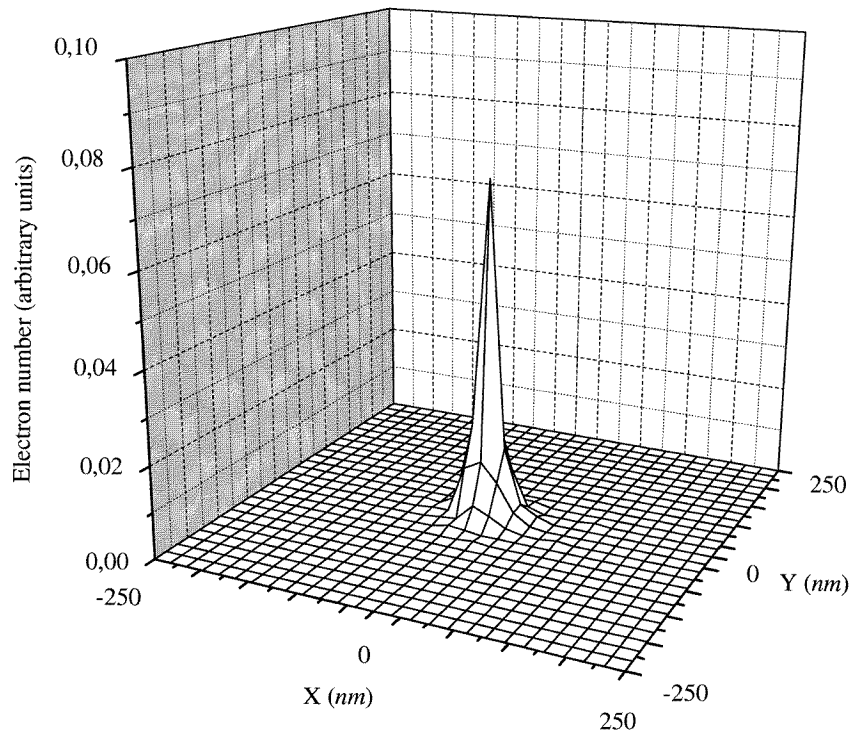


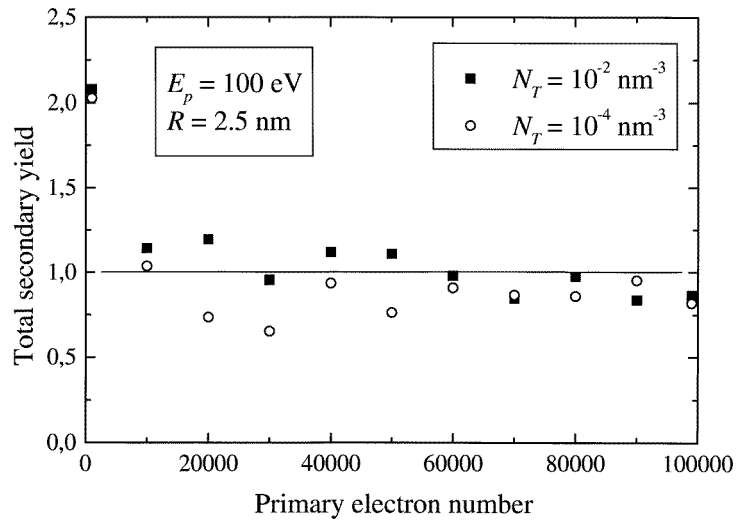
**Figure 7.** Spatial distribution of the electrons attracted back to the surface.

change during the charging up of the target.

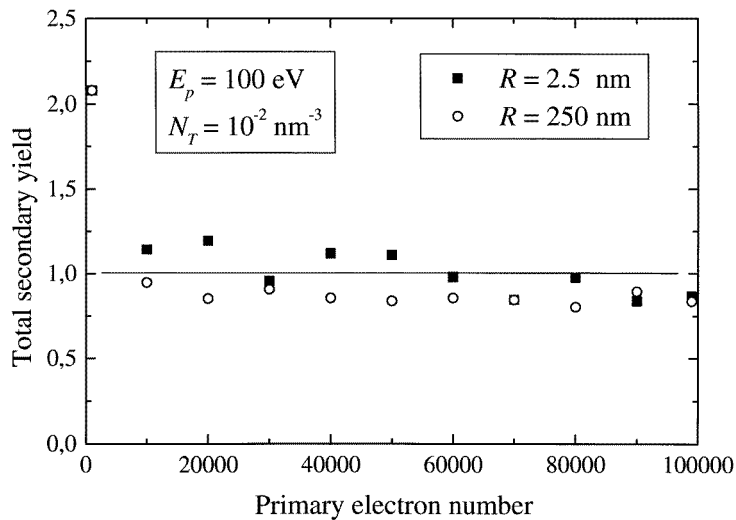
The spatial distribution of the electrons that are attracted back to the target surface is quite different (figure 7). It is representative of the size of the ring of negative charges which has formed close to the surface. One can notice that the ‘landing’ of the electrons mainly occurs under the primary spot (the spatial distribution decreases practically exponentially from the centre of the spot). However, as already mentioned, in this region the electrons recombine with the holes which are there in a majority.

For a PMMA target, Ying and Thong [22] have predicted theoretically the formation of rings of negative charges around a core region. This latter corresponds approximately to the primary spot area. At the beginning of the simulation, it is positively charged. However, according to their model, the accumulation of the negative charges at the core periphery leads to a negative drift of the core potential. In the absence of charge redistribution, this drift would increase continuously whereas, in our model, a stabilization is predicted. Ying and Thong have investigated the possibility of a surface breakdown followed by a redistribution of the charges at the core periphery whenever the local field exceeds some critical value. In that case the surface potential fluctuates randomly around a negative equilibrium value with discontinuities appearing as breakdown occurs. According to this model, the evolution of the surface potential results in momentary increases of the secondary yield followed by a relaxation. This has not been observed experimentally.

*3.2.3. Influence of some physical parameters.* The self-regulation effect is quite general. We have been able to confirm this behaviour in our simulations of the secondary emission



(a)



(b)

**Figure 8.** Influence on the total secondary yield evolution of the density of trapping sites (a) and of the primary spot diameter (b).

of  $\text{SiO}_2$ , for a large set of experimental situations. They concern the density of traps ( $N_T = 10^{-4}$  or  $10^{-2} \text{ nm}^{-3}$ ) and the focusing conditions ( $R = 2.5$  or  $250$  nm). When the target charges negatively, the resulting potential can cause a divergence of the primary electron beam at the surface and a broadening of the spot size. In the present case, the sample charges positively and such effects have not to be considered. One observes that varying the density of trapping sites  $N_T$  (figure 8(a)) or changing the spot diameter by modifying  $R$  (figure 8(b)) does not affect the yield limit.

The spatial distribution of the surface potential is difficult to relate to a particular parameter.  $V_s$  depends on the distribution of the charges, which itself depends on the

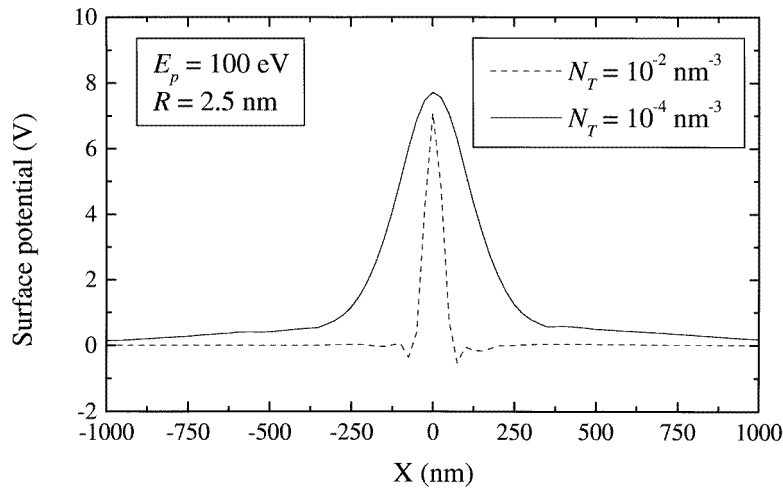


**Figure 9.** Influence on the surface potential distribution of the density of trapping sites.

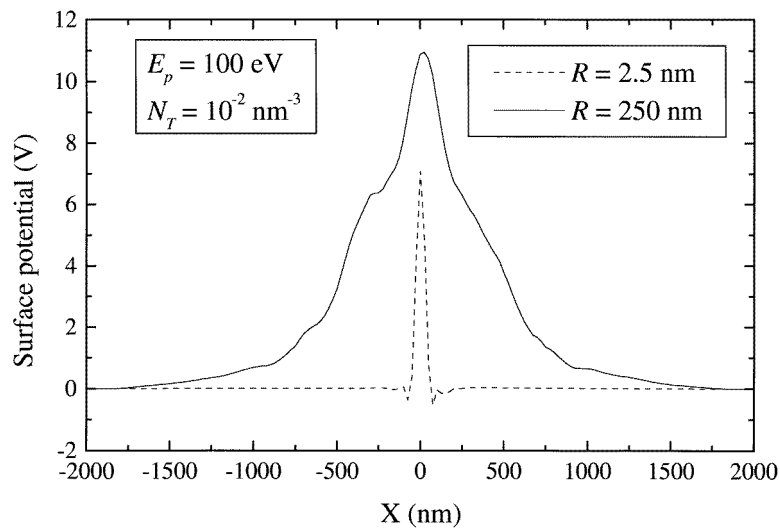


**Figure 10.** Influence on the surface potential distribution of the primary spot diameter.

polarizability of the medium and on the whole set of interaction scattering cross sections. The precise kinetics of the process depends also on the microscopic mobilities for which completely reliable values are not known. As already indicated, the asymptotic behaviour of the surface potential (like for the yield) depends only little on the primary energy.

Figure 9 shows the evolution of the surface potential distribution with the density of trapping sites. When  $N_T$  varies from  $10^{-4}$  to  $10^{-2} \text{ nm}^{-3}$ , the maximum value of  $V_s$  remains practically unchanged. However, the surface potential profile of course broadens, as the charges have to travel higher distances before being trapped.

As shown in figure 10, defocusing the primary beam by increasing  $R$  (from 2.5 to 250 nm) leads to a similar broadening. However, as shown in figure 11, for a sufficiently defocused beam, it is no longer possible to discern the effect of a variation of the trapping

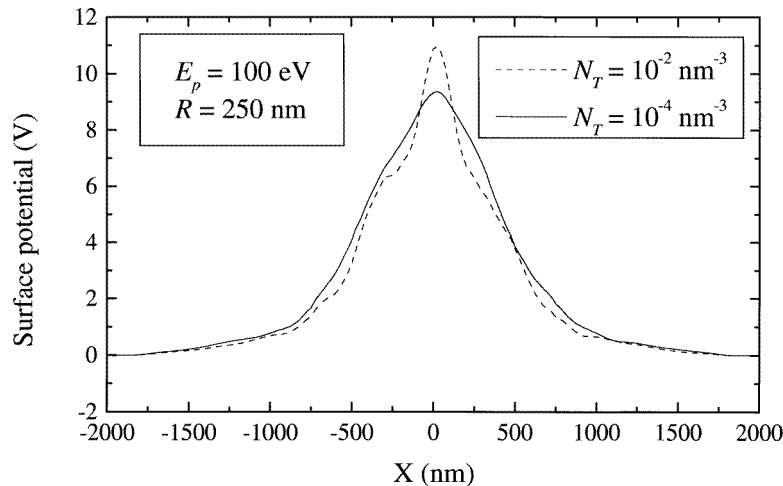


Figure 11. Same comments as for figure 9, but for a defocused beam.

site density on the profile of  $V_s$ , as the diffusion lengths before trapping become much lower than the spot size.

#### 4. Conclusions

In the primary energy range which has been studied in the present paper, the insulating target charges positively and the low energy electrons are attracted back to the surface. This results in a self-regulation of the total secondary yield and of the surface potential.

The building up of the space charge has been explained by the trapping of the charge carriers, which have acquired a large effective mass from their polarizing interaction with the surrounding medium. It would be important in the future to examine more precisely the microscopic aspects of these interaction mechanisms in order to clarify their role in the transport and in the secondary emission. Of course, the possibility for the charges to be detrapped under the influence of a temperature increase or due to some high values of the local electric field or even by ionization by electron impact has to be accounted for. This would be important to check for the stability of the space charge, for instance. These studies are in progress in our group.

#### Acknowledgments

Most of this work has been performed with the financial support of the French 'Centre de l'Energie Atomique' (CEA/DAM). The authors would like to thank this institution for its help.

#### References

- [1] Ganachaud J-P, Attard C and Renoud R 1997 *Phys. Status Solidi* b **199** 175
- [2] Attard C and Ganachaud J-P 1997 *Phys. Status Solidi* b **199** 455
- [3] Pendry J B 1974 *Low Energy Electron Diffraction (Techniques of Physics Series 2)* ed G K T Conn and K R Coleman (New York: Academic)

- [4] Ganachaud J-P 1977 *Thèse d'Etat* Université de Nantes
- [5] Devooght J, Dehaes J-C, Dubus A, Cailler M and Ganachaud J-P 1991 *Particle Induced Electron Emission I* (*Springer Tracts in Modern Physics* 122) ed G Höhler and E A Niekisch (Berlin: Springer) p 67
- [6] Gryzinski M 1965 *Phys. Rev. A* **138** 305–336
- [7] Fröhlich H 1954 *Adv. Phys.* **3** 325
- [8] Bradford J N and Woolf S 1991 *J. Appl. Phys.* **70** 490
- [9] Akkerman A, Boutboul T, Breskin A, Chechik R and Gibrekhterman A 1994 *J. Appl. Phys.* **76** 4656
- [10] Austin I G and Mott N F 1969 *Adv. Phys.* **18** 41
- [11] Blaise G 1992 *Vide Couches Minces Suppl.* **260** 1
- [12] Blaise G and Le Gressus C 1991 *J. Appl. Phys.* **69** 6334
- [13] Shluger A L and Stoneham A 1993 *J. Phys.: Condens. Matter* **5** 3049
- [14] Hachenberg O and Brauer W 1959 *Adv. Electron.* **11** 413
- [15] Seiler H 1983 *J. Appl. Phys.* **54** R1
- [16] Vicario E, Rosenberg R and Renoud R 1994 *Surf. Interface Anal.* **22** 115
- [17] Renoud R 1995 *Thèse de Doctorat* Université Lyon I
- [18] Renoud R, Rosenberg N and Vicario E 1995 *IEEE Annu. Rep.* p 175
- [19] Hugues R C 1979 *Phys. Rev. B* **19** 5318
- [20] Cazaux J, Kim K H, Jbara O and Salace G 1991 *J. Appl. Phys.* **70** 960
- [21] Cazaux J 1986 *J. Appl. Phys.* **59** 1418
- [22] Ying M H and Thong J T L 1994 *Meas. Sci. Technol.* **5** 1089